

1990

## THE PHOBOS LOW ENERGY TELESCOPE CHARGED PARTICLE EXPERIMENT

R.G. MARSDEN<sup>1)</sup>, V.V. AFONIN<sup>2)</sup>, A. BALAZS<sup>4)</sup>, G. ERDÖS<sup>4)</sup>, J.P.G. HENRION<sup>1)</sup>,  
A.K. RICHTER<sup>3)</sup>, P. RUSZNYAK<sup>4)</sup>, A. SOMOGYI<sup>4)</sup>, S. SZALAI<sup>4)</sup>, A. VARGA<sup>4)</sup>,  
L. VARHALMI<sup>4)</sup>, K.-P. WENZEL<sup>1)</sup> and M. WITTE<sup>3)</sup>

<sup>1)</sup> Space Science Department of ESA, ESTEC, Noordwijk, The Netherlands

<sup>2)</sup> Space Research Institute, Moscow, USSR

<sup>3)</sup> Max-Planck-Institut für Aeronomie, Lindau, FRG

<sup>4)</sup> Central Research Institute for Physics, Budapest, Hungary

Received 25 May 1989

The Low Energy Telescope (LET) experiment on board the Phobos 1 and 2 spacecraft measures the flux, energy spectra and elemental composition of solar energetic particles and cosmic ray nuclei from hydrogen up to iron in the energy range  $\sim 1$  to  $\sim 75$  MeV/n. The LET sensor system comprises a double  $dE/dX$  vs  $E$  solid-state detector telescope surrounded by a cylindrical plastic scintillator anticoincidence shield, and the instrument is equipped with a comprehensive particle identifier and event priority system that enables rare nuclei to be analysed in preference to the more common species. Isotope separation for light nuclei such as He is also achieved. The sensor is mounted on a rotating platform to enable coarse anisotropy measurements of low energy protons to be made.

### 1. Introduction

Measurements of solar energetic particles and low energy cosmic rays made by instruments on board the two Soviet Phobos spacecraft contribute to the study of the propagation and acceleration of charged particles on the Sun and in interplanetary space during the rising phase of solar cycle 22. This period is of particular interest since it coincides with the transition between the steady, recurrent solar wind flow patterns characteristic of solar minimum, and the transient flows, often related to energetic flare events on the Sun, encountered at solar maximum. The instrument described in this paper, the Low Energy Telescope (LET), is part of the ESTER experiment package on board Phobos [1] that has been designed to make measurements of the solar wind, the suprathermal and energetic particle populations, and low energy cosmic rays.

Specifically, the LET experiment measures the flux, energy spectra and elemental composition of solar energetic particles and low energy cosmic ray nuclei from hydrogen up to iron. The instrument covers an energy range from  $\sim 1$  to  $\sim 75$  MeV/n, using a double  $dE/dX$  vs  $E$  solid-state detector telescope surrounded by a cylindrical plastic scintillator anticoincidence shield. A comprehensive particle identifier and event priority system enables rare nuclei to be analysed in preference to the more common species, and isotope separation for

light nuclei such as He is also achieved. The sensor is mounted on a rotating platform to enable coarse directional measurements of low energy protons to be made.

The paper is organized as follows. In section 2 we describe the LET experiment hardware, including a brief discussion of the thermal design. Section 3 deals with the performance of the LET in flight, illustrated by an example of data obtained during the cruise phase. Concluding remarks are contained in section 4.

### 2. Instrumentation

The LET experiment hardware, which is identical on both Phobos spacecraft, comprises three elements: the LET sensor unit itself; a rotating platform on which the sensor is mounted in order to permit coarse directional information to be obtained on the 3-axis stabilised spacecraft; the LET Interface Unit (LIU). A block diagram of the complete LET instrument is shown in fig. 1. All three components are attached to a common mounting frame that also accommodates the ESTER SLED experiment [2]. The LET flight instrument, shown in the photograph of fig. 2, weighs 6 kg (excluding mounting frame and thermal hardware) and has an average power consumption of 2.5 W. The electrical interface to the spacecraft is provided by the ESTER Data Processing Unit (DPU-B) [1].

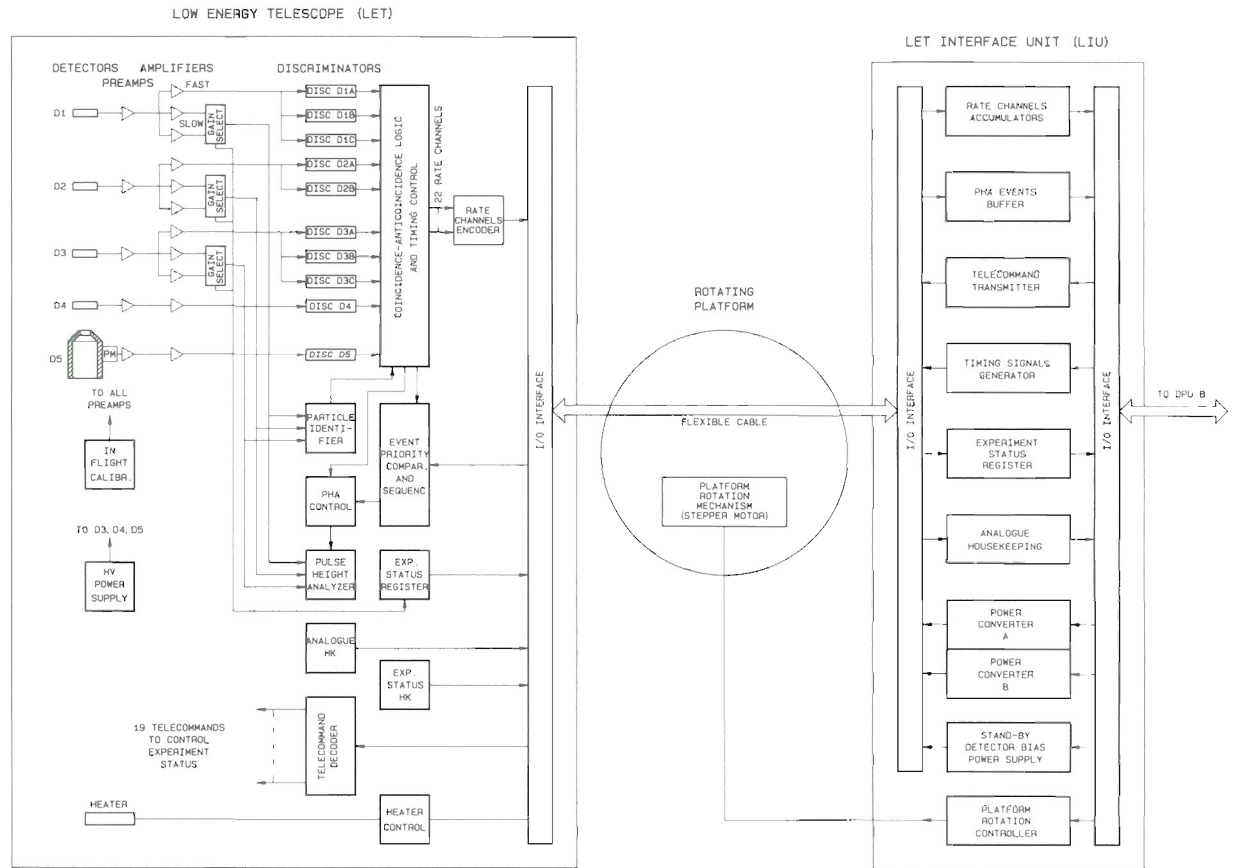


Fig. 1. Block diagram of the LET experiment, including the LET sensor, the rotating platform and the LET interface unit.

### 2.1. LET sensor

The LET sensor consists of a four-element solid-state detector telescope surrounded by a cylindrical plastic scintillator anticoincidence shield, together with its associated analog electronics. The telescope is shown in schematic form in fig. 3. Detectors D1 and D2 are large-area ( $6 \text{ cm}^2$ ) surface barrier devices having nominal thicknesses of  $30 \mu\text{m}$  (D1) and  $100 \mu\text{m}$  (D2), while D3 and D4 are  $2000 \mu\text{m}$  thick Li-drifted devices of  $10.0$  and  $12.5 \text{ cm}^2$  active area, respectively. D4 forms part of the anticoincidence shield. Relevant physical parameters for the detectors used in the flight sensors are given in table 1. The aperture of the telescope is covered by two thin foils, an inner Ti foil ( $2 \mu\text{m}$ ) and an outer Kapton foil ( $8 \mu\text{m}$ ), included for electrical screening and thermal control purposes, respectively. The telescope geometrical factor, defined by two circular collimators mounted in front of D1 and D2 in order to reduce unwanted edge effects, has a value of  $0.58 \text{ cm}^2 \text{ sr}$  for the coincidence channels. Low resolution single-detector (D1 only) measurements of protons and alpha

particles are also made. In this case, the geometrical factor is  $\sim 4 \text{ cm}^2 \text{ sr}$ .

The signals from detectors D1, D2 and D3 are fed into individual amplifier chains consisting of a charge-sensitive preamplifier followed by a parallel combination of three pulse-shaping voltage amplifiers (PSAs). To accommodate the large dynamic range required, separate low- and high-gain PSAs have been used, selected via an analog switch controlled by the third (fast) PSA in conjunction with a discriminator. The selected outputs are fed into a common 10-bit (1024-channel) ADC that provides pulse height information. The fast PSAs are followed by a number of threshold discriminators, the outputs of which are used in the coincidence logic to define a series of counting rate channels.

In addition, the outputs of the slower PSAs are fed into a Particle Identifier (PI) circuit that provides both counting rate and event priority information. The LET PI circuit makes it possible to obtain the counting rates corresponding to groups of nuclear species, and comprises a set of analog function generators and dis-

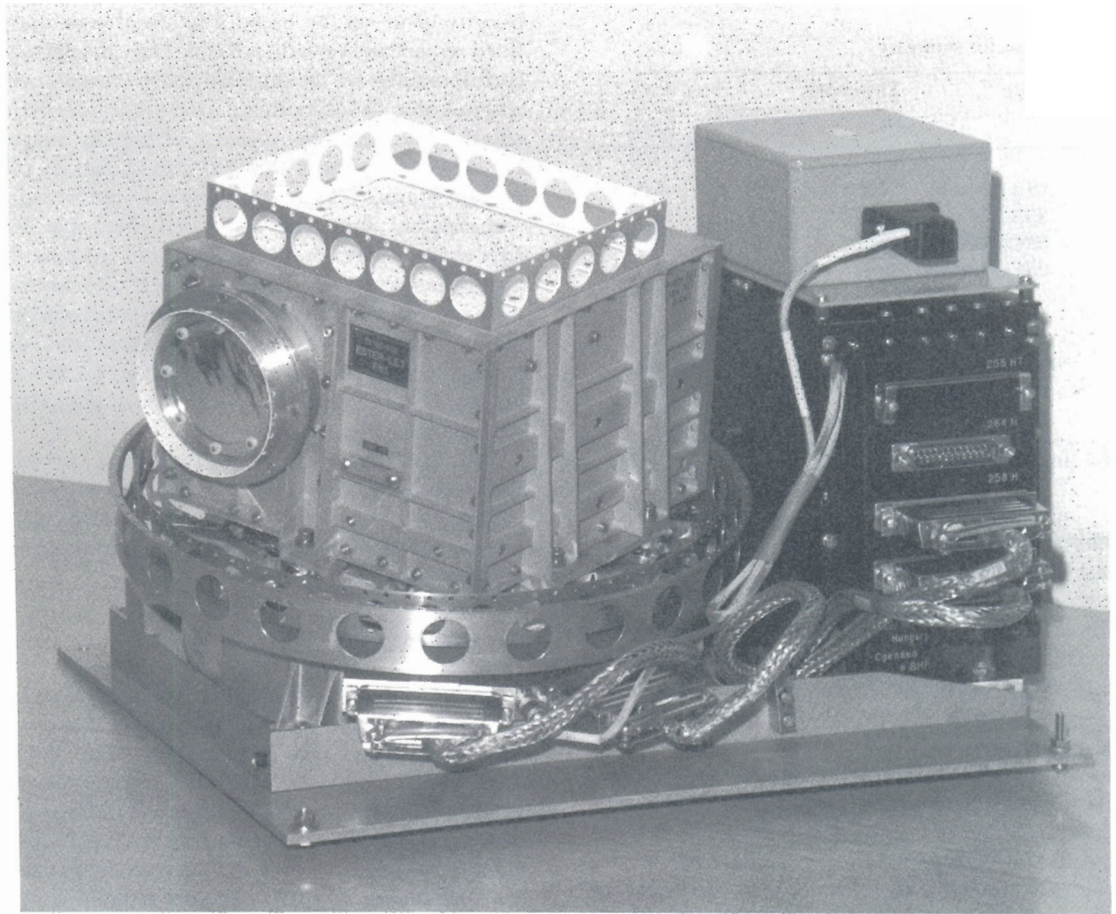


Fig. 2. The LET experiment configuration, showing the LET sensor unit, rotating platform and LIU, mounted on the common ESTER mounting frame.

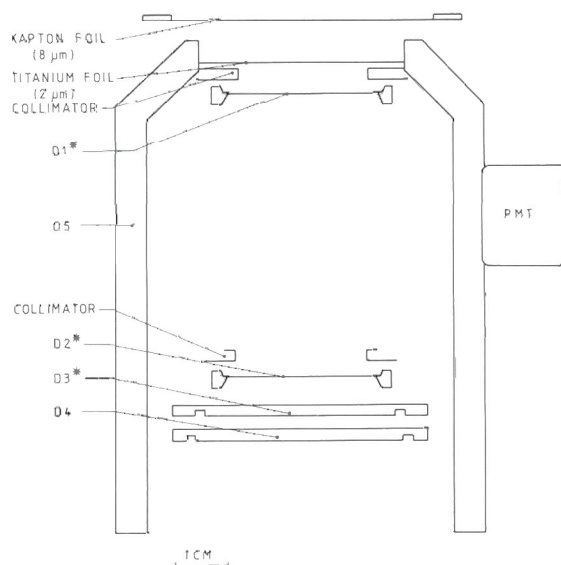


Fig. 3. Schematic representation of the LET detector telescope.  $Dm^*$  denotes a pulse height analysed detector

criminators that divide the instrument response into regions of different nuclear charge. The actual analog functions used are of two types, namely

$$E1 + b_i E2 = a_i, \quad (1)$$

and

$$E2(b_i + E3) = a_i, \quad (2)$$

where  $E1$ ,  $E2$  and  $E3$  are the energies deposited in detectors  $D1$ ,  $D2$  and  $D3$ , respectively, and  $a_i$ ,  $b_i$  are constants. For particles stopping in  $D2$ , the loci of points satisfying eq. (1) for given pairs of  $(a_i, b_i)$  values define boundaries on the  $\Delta E (\equiv E1)$  vs residual  $E (\equiv E2)$  diagram that separate the tracks corresponding to different elements or groups of elements into so-called "charge groups". The charge groups defined for the  $D1$ - $D2$  range are: protons; ( $^3\text{He}$ ,  $^4\text{He}$ ); (Li, Be, B); (C, N, O);  $Z \geq 10$  nuclei. In a similar way, charge group boundaries for particles stopping in  $D3$  are defined by eq. (2) with suitable pairs of  $(a_i, b_i)$  values. A different functional form is required in this case because of the

Table 1  
Phobos LET detector summary

Detector	Type <sup>a)</sup>	Thickness		Area [cm <sup>2</sup> ]
		[μm]	[mg/cm <sup>2</sup> ]	
Phobos-1				
D1	SSB (Ortec)	27.6	6.43	6.0
D2	SSB (Ortec)	95.2	22.18	6.0
D3	Si(Li)(LBL)	2038	474.8	10.0
D4	Si(Li)(LBL)	2000	466	12.5
Phobos-2				
D1	SSB (Ortec)	28.7	6.69	6.0
D2	SSB (Ortec)	103.8	24.19	6.0
D3	Si(Li)(LBL)	2031	473.2	10.0
D4	Si(Li)(LBL)	2000	466	12.5

<sup>a)</sup> SSB – silicon surface barrier.

pronounced curvature of the  $\Delta E$  vs residual  $E$  tracks resulting from the large thickness of D3 relative to D2. The same charge groups as before are defined for the D1–D2–D3 range, with the addition of a high  $Z$ -group corresponding to  $Z \geq 20$ . The boundaries corresponding to the (C, N, O) charge group are illustrated schematically in figs. 4 and 5 for the D1–D2 and D1–D2–D3 ranges, respectively.

Each of the charge groups has an associated counting rate register which is incremented each time a valid event within the group is observed. Accumulation intervals are 236 s for the proton and alpha particle rate channels and 1180 s for the heavy ion rate channels. In addition to providing counting rate information, the PF output is used to generate a 4-bit event code that controls the Event Priority System. The latter is included in order to maximise the LET PHA data-collection efficiency for the rarer nuclear species in the cosmic ray flux. Such a system is needed because the LET telemetry allocation (2.4 bits per s) limits the number of PHA events that can be transmitted to 2 per minute. Each pulse-height-analysed event is assigned a 4-bit

priority value on the basis of its event code via predefined sequences stored in a ROM. Only the pulse heights corresponding to the highest-priority event occurring within every 30 s sampling period are transferred to the telemetry stream. The sequence of priority assignments for all event codes is changed periodically in order to prevent biasing effects. In addition to pulse height data and proton, alpha and heavy ion rates, the 360-byte LET data frame contains digital status information and analog housekeeping values, as well as counting rate data for the individual detectors. Housekeeping information includes instrument voltages, the detector leakage currents and temperature values for the detector telescope and electronics. A summary of the LET digital data channels is given in table 2.

Also included in the instrument is an In-Flight Calibrator (IFC) circuit that checks, on command, the electrical characteristics of the instrument by delivering a sequence of pulses having well-defined amplitudes to all amplifier inputs.

## 2.2. Rotating platform

In order to measure the directional characteristics of the particle fluxes, the LET sensor is mounted on a rotating platform. The full rotation range of the platform (175°) is adjusted so that in the extreme positions, the sensor axis is oriented close to the average direction of the interplanetary magnetic field. This range is divided into steps of 44°, data accumulation occurring for a fixed period of 236 s at each of the five positions. In normal operation, the platform makes a complete  $+60^\circ$  (with respect to the spacecraft  $X$ -axis)  $\rightarrow -115^\circ \rightarrow +60^\circ$  scan cycle in 40 min, corresponding to two telemetry periods. The scan plane of the platform is tilted with respect to the ecliptic by  $12^\circ$  in order to avoid obscuring the LET field-of-view by other payload elements.

The main components of the platform unit are a stepper motor and its associated transmission gear that

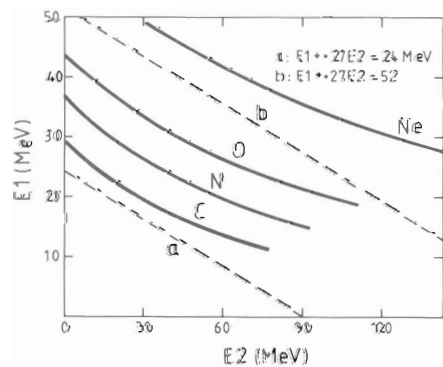


Fig. 4. LET particle identifier boundaries (dashed lines) plotted for (C, N, O) groups events stopping in D2.

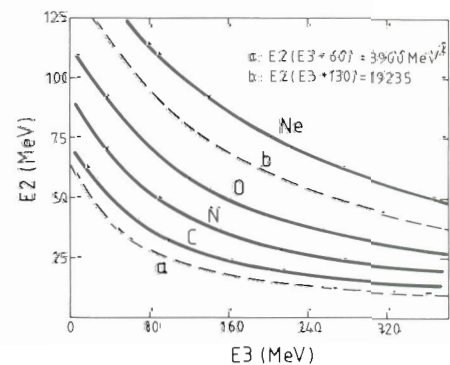


Fig. 5. As for fig. 4, but for particles stopping in D3.

Table 2  
Phobos LET data channel summary

Channel no.	Code	Measurement	Time resolution [s]
1	P1	proton 0.9–1.2 MeV	240
2	P2	1.2–3.0	240
3	P3	1.8–3.8	240
4	P4	3.8–8.0	240
5	P5	9.0–19	240
6	A1	alpha 1.0–5.0 MeV/n	240
7	A2	1.9–4.0	240
8	A3	4.0–9.0	240
9	A4	9.0–19	240
10	H1	Li, Be, B 2.3–5.2	1200
11	H2	5.2–56	1200
12	H3	C, N, O 3.2–7.5	1200
13	H4	7.5–39	1200
14	H5	Z ≥ 10 3.9–9.5	1200
15	H6	9.5–50	1200
16	H7	Z ≥ 20 12.–75	1200
17	E1	e <sup>-</sup> 0.35–1.5 MeV	1200
18	S1	D1 singles	600
19	S2	D2 singles	600
20	S3	D3 singles	600
21	S4	D4 singles	600
22	S5	D5 singles	600
	PHA	pulse heights/flags LET status	30 1200

drives the circular platform which is supported at its rim by two rows of Delrin ball-bearings. Two flexible cables, consisting of two layers of printed copper tracks enclosed in three layers of 50  $\mu\text{m}$  Kapton foil, are wrapped around the axis of the platform and provide the electrical connection between the LET and LIU. A high precision potentiometer delivers accurate (better than 0.5%) measurements of the platform position, and end-switches followed by mechanical stops are incorporated to prevent rotation beyond the  $+60^\circ$  or  $-115^\circ$  positions.

During flight, the platform, which is controlled by DPU-B via the motor drive circuitry incorporated in the LIU (see below), can be operated in two modes: normal mode and high power mode. In normal mode, the platform moves between each of the five pointing positions in 4 s; in high power mode, a higher (by a factor 4) motor torque is provided, and the travel time between positions is correspondingly longer. This latter mode is included for operation under special conditions (test, platform malfunction, extreme temperatures, etc.). The platform can also be commanded to move directly

to either end position, stopping once it reaches  $+60^\circ$ , or starting the normal scan from the  $-115^\circ$  position.

### 2.3. LET interface unit (LIU)

The LET Interface Unit, as the name implies, serves as the interface between the LET analog electronics and the ESTER DPU-B (see fig. 1). The unit is physically separate from the LET sensor and, as mentioned above, also houses the motor drive control electronics for the platform. Functionally, the LIU comprises: the LET rate channel and PHA digital data interfaces; the telecommand and status interfaces; the analogue housekeeping interface and the power supply interface. In addition, the LIU provides the timing signals necessary for correct operation of the LET.

### 2.4. LET thermal design

The thermal design is driven by two contradictory boundary conditions, namely (1) temperature extremes of  $-20^\circ$  and  $+50^\circ\text{C}$  are to be expected for equipment mounted on the spacecraft body, and (2) the operating temperature of the solid-state detectors should never exceed  $+35^\circ\text{C}$  (danger of irreversible damage). These constraints dictate that the LET sensor unit be thermally isolated from the rotating platform and other structural elements. Thermal control is then achieved as follows: the power dissipated inside the LET sensor ( $\sim 2$  W) is radiated to space through a ca. 100  $\text{cm}^2$  white-painted radiator surface on top of the sensor box, while a 0.5 W heater prevents excessive cooling. This thermal design has proven to be very effective in flight, and the detector telescope is maintained at a stable temperature ranging between  $-5^\circ$  and  $+10^\circ\text{C}$ .

## 3. LET performance in flight

The Phobos spacecraft 1 and 2 were successfully launched from the Baikonur Cosmodrome on 7 and 12 July 1988, respectively. Following a period of ca. 12 days to allow for outgassing, the LET experiments were switched on on 19 July, 00:30 UT (Phobos 1) and 25 July, 05:59 UT (Phobos 2). Initial data showed that the LET sensors on both spacecraft were functioning nominally, although the rotating platform on Phobos 1 was apparently unable to move from the  $-115^\circ$  launch position. Attempts to free the platform by telecommand were unsuccessful, and the condition persisted up to the end of August 1988, at which time radio contact with Phobos 1 was lost. As an example of the data obtained on Phobos 2 during the cruise phase from Earth to Mars, fig. 6 shows pulse height information plotted in the  $\Delta E$  vs residual  $E$  format for particles stopping in D2. The data cover a 4 d period starting at 00:00 UT on

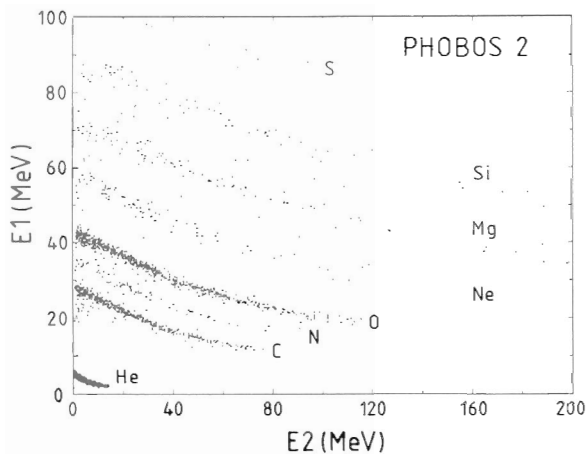


Fig. 6. Flight data from the LET experiment on Phobos 2. Shown is the D1 vs D2 pulse height matrix for the solar flare event of 17–20 December 1988.

17 December 1988, and represent particles of solar origin that have been accelerated during solar flare events and transported out to the location of Phobos 2. The tracks corresponding to the different nuclear species are clearly seen. By normalising the pulse height data to the total number of counts registered in each charge group rate accumulator, the relative abundance and energy spectrum of each individual element may be derived.

In addition to the flight data, a substantial database on the performance of the LET has been accumulated during ground testing. The LET sensors for the Phobos mission are, with the exception of the interface to the DPU, largely identical to the Low Energy Telescope to be flown on the much-delayed Ulysses mission [3]. In particular, the detector telescopes have the same specifications as the Ulysses LET instrument. The latter has already been extensively calibrated at particle accelerator facilities, with exposures to both heavy ion and proton beams [4–6].

#### 4. Conclusions

The performance of the LET instruments on the multidisciplinary Phobos mission has matched that expected from ground calibration and test, and the experiments will make important contributions to our knowledge of the particle populations in interplanetary space during the transition phase between solar minimum and solar maximum. Furthermore, based on the measured performance of the Phobos flight hardware, the LET experiment on the exploratory Ulysses mission to the solar poles is confidently expected to provide high-quality data following its launch in 1990.

#### Acknowledgements

Institutes collaborating on the LET experiments are the Space Science Department of ESA, the Space Research Institute, Moscow, the Central Research Institute for Physics, Budapest, and the Max-Planck-Institut für Aeronomie, Lindau. The authors wish to express their thanks to all those who have contributed to the success of the experiments. In particular, from ESA/SSD, L. Smit, J.M. Bouman, J. Fleur and J. Dalcolmo; from MPAe, U. Strohmeyer, K. Fischer and W. Engelhardt; from CRIP, A. Steiner, I.T. Szücs and J. Erö; from IKI, S. Gubsky and V. Semenova.

#### References

- [1] V. Afonin et al., this issue, *Nucl. Instr. and Meth. A290* (1990) 223.
- [2] S. McKenna-Lawlor et al., this issue, *Nucl. Instr. and Meth. A290* (1990) 217.
- [3] K.-P. Wenzel, R.G. Marsden, D.E. Page and E.J. Smith, *Adv. Space Res.* 9 (1989) 425.
- [4] R. Kamermans, J. Henrion, R.G. Marsden, T.R. Sanderson and K.-P. Wenzel, *Nucl. Instr. and Meth.* 171 (1980) 87.
- [5] J.F. LeBorgne, J. Henrion, R.G. Marsden, T.R. Sanderson and K.-P. Wenzel, Report ESA STM-224 (1981).
- [6] R.G. Marsden, J. Henrion, T.R. Sanderson, K.-P. Wenzel, N. de Bray and H.P. Blok, *Nucl. Instr. and Meth.* 221 (1984) 619.